

Ultimate strength behavior of steel-concrete-steel sandwich beams with ultra-lightweight cement composite, Part 1: Experimental and analytical study

Jia-Bao Yan^a, J.Y. Richard Liew^{*}, Min-Hong Zhang^b and Junyan Wang^c

Department of Civil and Environmental Engineering, National University of Singapore, E1A-07-03, One Engineering Drive 2, Singapore 117576

(Received December 13, 2013, Revised April 04, 2014, Accepted April 20, 2014)

Abstract. Ultra-lightweight cement composite (ULCC) with a compressive strength of 60 MPa and density of 1450 kg/m³ has been developed and used in the steel-concrete-steel (SCS) sandwich structures. ULCC was adopted as the core material in the SCS sandwich composite beams to reduce the overall structural weight. Headed shear studs working in pairs with overlapped lengths were used to achieve composite action between the core material and steel face plates. Nine quasi-static tests on this type of SCS sandwich composite beams were carried out to evaluate their ultimate strength performances. Different parameters influencing the ultimate strength of the SCS sandwich composite beams were studied and discussed. Design equations were developed to predict the ultimate resistance of the cross section due to pure bending, pure shear and combined action between shear and moment. Effective stiffness of the sandwich composite beam section is also derived to predict the elastic deflection under service load. Finally, the design equations were validated by the test results.

Keywords: cement composite; bond strength; connector; shear connector; sandwich structure; tension connector

1. Introduction

Steel-concrete-steel (SCS) sandwich composite structure consists of two external steel face plates and an internal concrete core using cohesive material or mechanical shear connectors to bond different components together at their interface and form a composite panel. Cohesive materials provide continuous bond along the member but the quality of the bond is affected by imperfections and thus it often affects the structural performance of SCS sandwich composite structure (Aboobucker *et al.* 2009). Mechanical shear connectors provide localized bonds at discrete points along the member depending on their spacing. Different types of shear connectors have been developed and used in the steel-concrete composite structure e.g., headed shear studs,

*Corresponding author, Professor, E-mail: ceeljy@nus.edu.sg

^a Research Fellow, E-mail: ceeyanj@gmail.com

^b Professor, E-mail: mhzhang@nus.edu.sg

^c Research Fellow, E-mail: ceewjy@nus.edu.sg

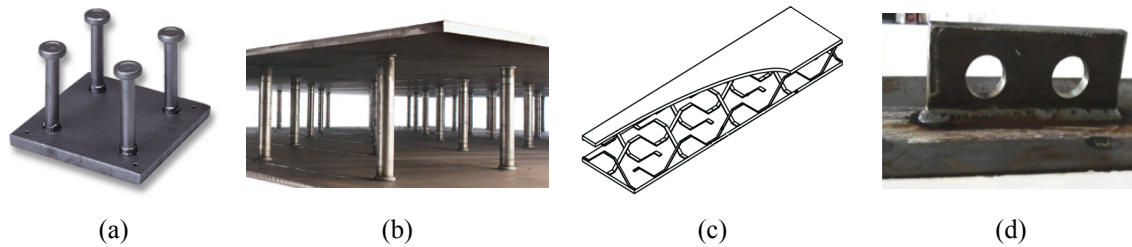


Fig. 1 Different types of mechanical shear connectors (a) headed shear studs; (b) friction welded connectors in 'bi-steel' structure; (c) corrugated strip connectors; (d) perfobond connectors

friction welded connectors in 'bi-steel' structure, corrugated strip connectors, perfobond connectors as shown in Fig. 1 (Xie *et al.* 2007, Leekitwattana *et al.* 2011, Kim *et al.* 2013). SCS sandwich composite structure with overlapped headed shear studs namely 'double skin' structure has been developed and studied in the past two decades (Narayanan *et al.* 1998, Shanmugam *et al.* 2002). The headed shear studs not only serve to transfer interfacial shear force and resist interfacial slip to achieve composite action, but also act as the shear links to provide transverse shear resistance. This type of structure has advantages of fast installation, permitting prefabrication, and providing satisfactory structural performances. It has potential to be used in nuclear containment structure, shear walls, tunnels, liquid and gas containers, and blast protection structures because of the strong and impermeable face plates (Wright *et al.* 1991). Headed shear studs have been widely studied and used in the steel-concrete composite structure and SCS sandwich structure (Chung and Lawson 2001, Shanmugam and Lakshmi 2001, Lam 2007, Mirza and Uy 2010). In the present study, overlapped headed shear studs were chosen for the SCS sandwich composite structure to develop slim decking for the use in marine and offshore structures.

Special lightweight concrete (LWC) type of core material was developed for steel-concrete-steel (SCS) sandwich composite structures in order to reduce the overall weight of SCS system making it was a competitive choice for marine and offshore structures (Liew and Sohel 2009). LWC consisting of expanded clay type of coarse aggregate with compressive strength 30 MPa and density 1450 kg/m^3 was used in SCS sandwich composite structure by Dai and Liew (2010), Sohel and Liew (2011). More recently, new high strength ultra-lightweight cement composite (ULCC) with density 1450 kg/m^3 and compressive strength 65 MPa has been developed (Wang *et al.* 2012, 2013, Sohel *et al.* 2012, Yan *et al.* 2014a, b). In the present study, ULCC was chosen as the core material to develop slim deck used in offshore and marine structure.

Steel-concrete-steel (SCS) sandwich composite beams with normal weight concrete (NWC) and headed shear studs has been investigated and a design guideline had been developed for the civil engineering applications (Oduyemi and Wright 1989, Narayanan *et al.* 1994, McKinley and Boswell 2002). Double skin slabs with normal strength concrete were tested by Kumar (2000). However, all these research activities were carried out on SCS sandwich composite structure with normal weight concrete. Research on this type of structure with ultra-lightweight concrete is not available.

In the present research, nine steel-concrete-steel sandwich composite beams were tested to investigate their load displacement behavior up to the maximum load. Parameters under investigation include thickness of the steel face plate, strength of core material, spacing of the connectors, and shear spans. Design equations were developed to predict the bending moment

resistance and transverse shear resistance of the cross section of the sandwich composite beam as well as elastic load-elastic deflection curves of the beams. The validity of the analytical method was established by comparing the predicted ultimate strength and load displacement responses with those from the tests. The analytical method may be used conservatively for the design of slim and lightweight SCS sandwich composite beam structure.

2. Test program

Nine steel-concrete-steel (SCS) sandwich composite beams (B1-B9) were prepared to investigate their structural performances. Overlapped headed shear studs were used to bond the core material and steel face plates. These nine beams were designed by varying the key parameters including (1) thickness of the steel face plates; (2) concrete strength and type; (3) spacing of the shear connectors; and (4) shear span of beam.

2.1 Core materials

Ultra-lightweight fiber-reinforced cement composite (ULCC) was developed with 28-day compressive strength above 60 MPa and density of 1450 kg/m^3 (Yan *et al.* 2014a, b). Compared with normal strength concrete with similar strength and density of 2400 kg/m^3 , the ULCC has a high specific strength (strength-to-density ratio) greater than $40 \text{ kPa}/(\text{kg/m}^3)$ versus $25 \text{ kPa}/(\text{kg/m}^3)$ for the former. ULCC exhibits comparable ultimate tensile and flexural strengths with conventional normal weight concrete (NWC) but with a 40% weight reduction. Due to its porous structure, the elastic modulus of ULCC is approximately 50% of conventional NWC. ULCC was made of ordinary Portland cement, silica fume, water, chemical admixtures, polyvinyl alcohol (PVA) fibers, and cenospheres with particle sizes ranging from 10 to $400 \mu\text{m}$ as shown in Fig. 2(a). The cenospheres are hollow alumino-silicate spheres obtained from fly ash from coal-burning power plants, and commercially available. The fibers had a length of 6 mm and a diameter of $27 \mu\text{m}$ to reduce the brittleness of the ULCC. Fresh ULCC is flowable and suitable for grouting the sandwich composite structures. Benefiting from the excellent workability, the ULCC can be pumped and less vibration is needed, which greatly increase the construction efficiency.

Lightweight concrete (LWC) was made of expanded clay lightweight fine aggregate with

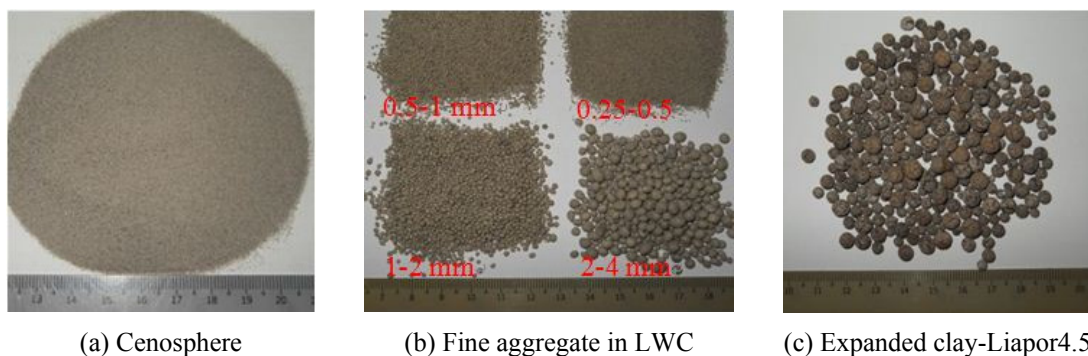


Fig. 2 Aggregates in ULCC and LWC

different diameters (Fig. 2(b)), expanded clay lightweight coarse aggregate (Fig. 2(c)), cement, and water. The expanded clay aggregate namely Liapor F4.5 was commercially available, and was used to produce LWC. This LWC was used in Beam B4 as the core material.

High performance concrete (HPC) was used in this experimental study for comparison. This HPC was a proprietary mixture made of cementitious materials, chemical admixtures, and fine mineral aggregate (bauxite). The density, compressive strength, and modulus of elasticity of the HPC were 2738 kg/m³, 180 MPa and 60 GPa, respectively. This HPC was used in Beam B5.

The mix proportions of ULCC, LWC, and HPC are as listed in Table 1.

2.2 Steel materials and connectors

Mildsteel plates were used to fabricate the SCS sandwich composite beams. Tensile coupon tests were performed on the steel plates to obtain the strengths and elastic modulus according to ASTM A370-05 (2005). The mechanical properties of the steel plates and headed shear studs are tabulated in Table 2.

Table 1 Mixture proportions of the concretes

Concrete	Water (kg/m ³)	Cement (kg/m ³)	SF* (kg/m ³)	FA* (kg/m ³)	FA type	CA* (kg/m ³)	CA Type	SP* (L/m ³)
LWC	175.0	500.0	0.0	127.0	LWFA ^a	315.0	F4.5 ^b	0.0
ULCC	259.4	741.0	65.0	335.0	CN ^c	-	-	7.7
HPC	202.1	-	-	2659.6	D4	-	-	-

*W/C = water to cement ratio; CA = Coarse aggregate; CN = cenosphere; FA = fine aggregate;

D4 = Ducorit®D4; LWFA = lightweight fine aggregate; SF = silica fume; SP = superplasticizer;

^aLWFA has a dry density of 503 kg/m³, ^bF4.5 has bulk density 450 kg/m³; ^cCN-cenosphere has a bulk density of 620 kg/m³

Table 2 Details of the SCS sandwich composite beams

Beam	t_c & t_s (mm)	S (mm)	L (mm)	Core material	f_c (MPa)	E_c (GPa)	u (kg/m ³)	f_y (MPa)	σ_u (MPa)
B1	4.0	100	500	ULCC	67.4	17.3	1441	275	527
B2	6.0	100	500	ULCC	65.2	17.3	1450	305	527
B3	12.0	100	500	ULCC	69.3	17.3	1450	310	527
B4	6.0	100	500	LWC	24.1	12.7	1324	305	527
B5	6.0	100	500	HPC	180.0	60.0	2672	305	527
B6	6.0	150	500	ULCC	67.2	17.3	1521	305	527
B7	6.0	200	500	ULCC	64.6	17.3	1440	305	527
B8	6.0	100	1100	ULCC	67.2	17.3	1521	305	527
B9	5.7	100	1600	ULCC	64.6	17.3	1440	310	527

* t_c = thickness of the steel plate under compression; t_s = thickness of the steel plate under tension; S = spacing of the connectors in the beam; L = span of the beam; E_c = secant modulus of elasticity; u = density of the concrete core; σ_u = ultimate tensile strength of the connectors; f_y = yield strength of the steel plates

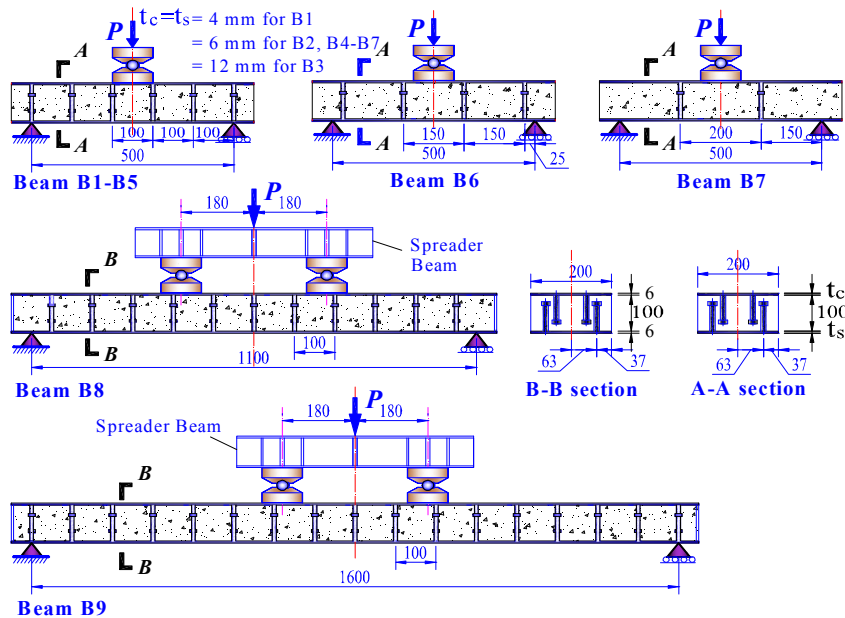


Fig. 3 Test setup and details of the sandwich beam

2.3 Details of specimens and test setup

Nine SCS sandwich composite beams were designed with the same cross section (width = 200 mm and height of the core material = 100 mm). The span length for specimens B1-B7 was 500 mm, whereas that for B8 and B9 was 1100 mm and 1700 mm, respectively. Headed shear studs with a diameter of 13 mm and length of 75 mm were used in the test beams. Different steel plate thicknesses, $t = 4, 8,$ and 12 mm, were used for beam B1, B2, and B3, respectively. Core materials with different strengths and type i.e., ULCC C60, LWC C30, and HPC C180 were used in B2, B4, and B5, respectively. Different spacing of the connectors $S = 100, 150,$ and 200 mm were used for Beam B2, B6, and B7, respectively. In order to investigate the influence of the shear spans, different beam spans $L_s = 500, 1100,$ and 1600 mm were designed for B2, B8, and B9, respectively. The details of the test beams are given in Table 2.

Quasi-static displacement-controlled-loading with a rate of 0.5 mm/min was applied to the beams. Beams B1-B7 were subjected to a concentrated load at the mid-span. B8 and B9 were tested under two-point loading in which a spreader beam was used to spread the concentrated load to two load cell with a distance of 180 mm off the mid-point as shown in Fig. 3.

Linear varying displacement transducers (LVDTs) were installed at the mid-point for B1-B7. For Beams B8 and B9, three LVDTs were installed at the mid-span and at two locations with 180 mm offset from the mid-point. One direction strain gauges were also installed at the both top and bottom steel plate at the mid-length cross section to measure the strains at different load levels.

3. Test results and discussions

3.1 Failure mode and ultimate strengths

Table 3 Ultimate strength and failure mode of the beam B1-B9

Beam	B1	B2	B3	B4	B5	B6	B7	B8	B9
Failure mode	CCSF, BSY	CCSF	CCSF, BSY	CCSF	CCSF	CSF, CCSF	CSF, CCSF	CCSF, BSY	FF, BSY
P_u (kN)	212.3	236	378	133.6	451.3	233.1	165.4	174.3	127.8

*BSY = Bottom steel plate yield; CCSF = concrete core shear failure; CSF = connector shear failure; FF = flexural failure; P_u = ultimate strength of the test; Cov = coefficient of variance.

Three main observed failure modes from the tests were flexural failure, transverse shear failure and combined failure of shear and flexure as shown in Figs. 4(a), (b), and (c), respectively.

For flexural failure, micro vertical cracks were observed initiated from the bottom flange and propagated to the top flange. The tension steel plate yielded and the structure exhibited a large and ductile deformation. For transverse shear failure, diagonal shear cracks were observed in the core material starting from the bottom flange and moved towards the loading point. At the final stage of loading, major shear cracks were observed in the core material bridging the loading point and the end support. For the combined failure mode, micro cracks were firstly developed in the pure bending region propagating from the bottom flange to the top flange as the beam deflected further. After the beam attained a certain degree deflection, it finally failed in diagonal shear tension.

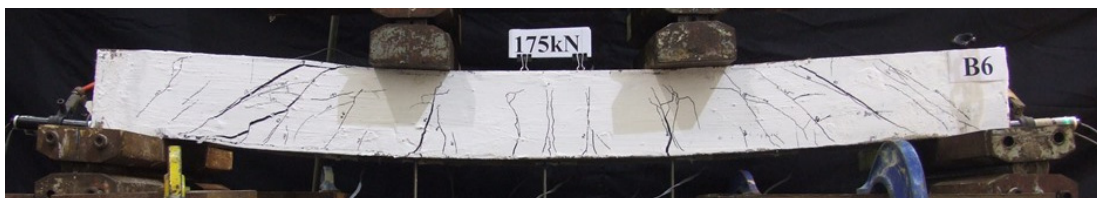
The ultimate strengths and failure modes of the beams were recorded as shown in Table 3.



(a) Flexural failure in B9



(b) Shear failure in B1 and B7



(c) Combined shear and flexural failure in B8

Fig. 4 Failure modes of SCS sandwich beam

3.2 Discussions

3.2.1 Effect of steel plate thickness

Steel plates thickness $t = 4, 6,$ and 12 mm were used for beams B1, B2, and B3, respectively. The influence of steel plate thickness on the load-deflection behavior and ultimate strength are shown in Fig. 5(a) and (b), respectively. It is observed that the use of thicker steel plate enhances the load carrying capacity of the SCS sandwich composite beam. This is because SCS sandwich composite beam with thicker steel plates offers higher bending moment resistance and transverse shear resistance of the cross section. The ultimate strength of the beam increases by about 11% and 78% when the thickness of the steel face plate increases from 4 mm to 6 mm and to 12 mm, respectively. The increase in the ultimate strength is almost linearly proportional to the thickness of steel face plate.

Yielding of the bottom steel plate was observed in Beams B1 and B3 as their failure were due to flexure. Yielding was not observed in Beam B2 as it failed in transverse shear rather than flexural bending.

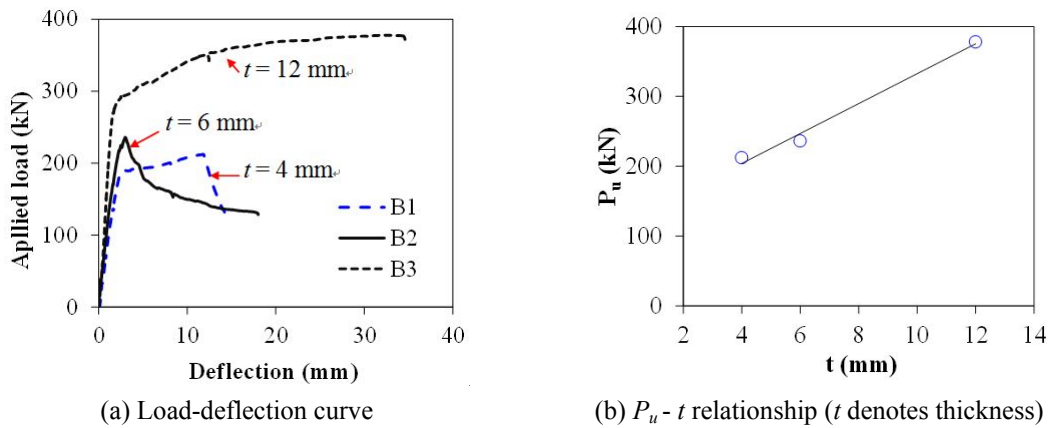


Fig. 5 Effect of steel plate thickness

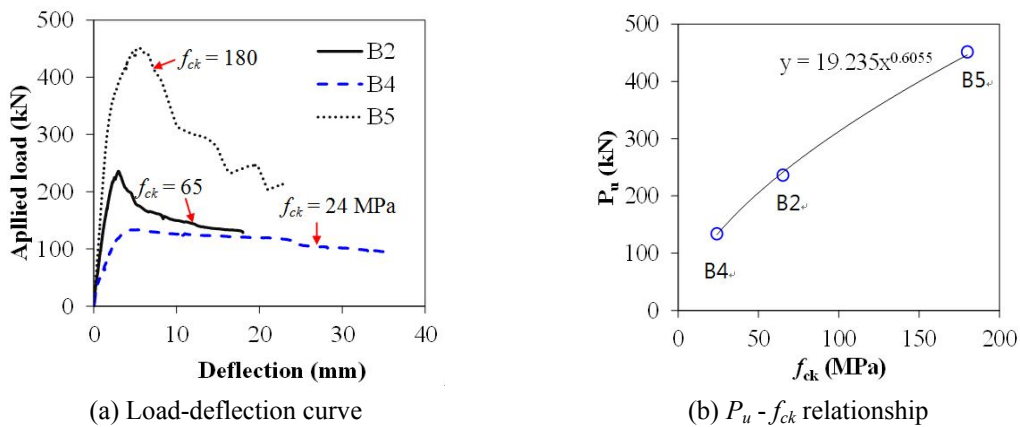


Fig. 6 Effect of strength of the core material

3.2.2 Effect of strength of core material

Beams B2, B4, and B5 were infilled with ULCC, LWC and HPC materials of compressive strength 65, 24 and 180 MPa, respectively. The effect of the strength of the core material on the load-deflection curves and ultimate strength of the SCS sandwich composite beams are shown in Figs. 6(a) and (b), respectively. It can be observed that all these three beams failed in a typical shear failure with a sudden drop of the load-deflection response. Since the three beams have the same steel plate thickness and same layout of the shear connectors, the ultimate resistance of the SCS sandwich composite beam was increased by 77 % and 238 % mainly due to the increase of the strength of the core material from 24 to 65 and 180 MPa, respectively. Since the shear resistance of the SCS sandwich composite beam is about 0.61 times of the compressive strength f_{ck} of the core material which is about 0.5 times that is used in the ACI 318 design code (2008). The shear resistance of the core material is determined by its tensile strength. Concrete with higher compressive strength offers higher tensile strength, which finally results in higher shear resistance of the beam.

It can be observed that SCS sandwich composite beams with higher strength core material exhibited higher elastic stiffness in the load-deflection curves. This is because higher strength concrete offers larger secant modulus of elasticity, which results in higher stiffness of the beam section.

3.2.3 Effect of spacing of connectors

Beams B2, B6, and B7 were made with connectors spaced at 100, 150, and 200 mm, respectively. The influence of the connectors' spacing on the load-deflection behaviors and ultimate strength of the beams are shown in Figs. 7 (a) and (b), respectively. It can be observed that B2 with 100 mm spacing of connectors exhibited ultimate load carrying capacity close to that of B6 with 150 mm spacing of connectors (See Table 3). This is because that the number of shear connectors that contributes to the shear resistance within the shear span is the same for these two beams. There are four pairs of connectors in specimens B2 and B6 within the shear span although their connector's spacing is different.

The shear strength of the beam B7 with connector spacing 200 mm is decreased by 30% compared to B2 with 100 mm connector spacing. However, for B7 ($S = 200$ mm) only four pairs

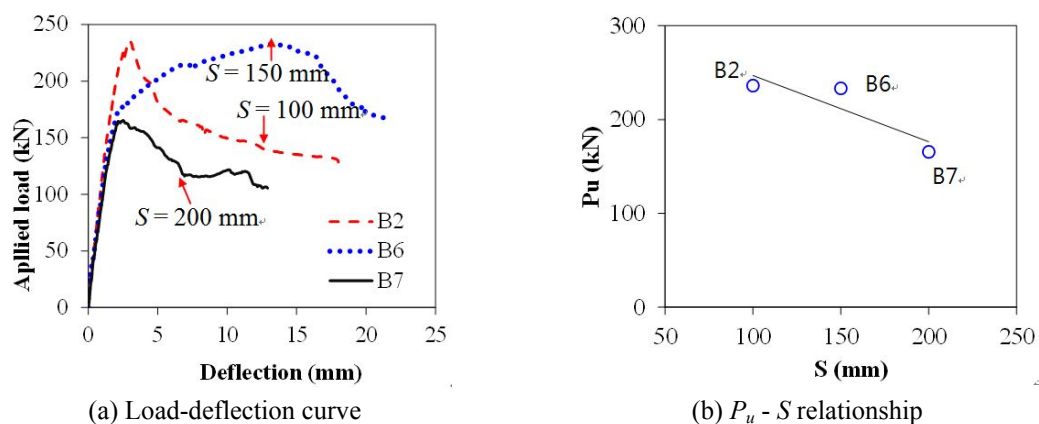


Fig. 7 Effect of connector's spacing

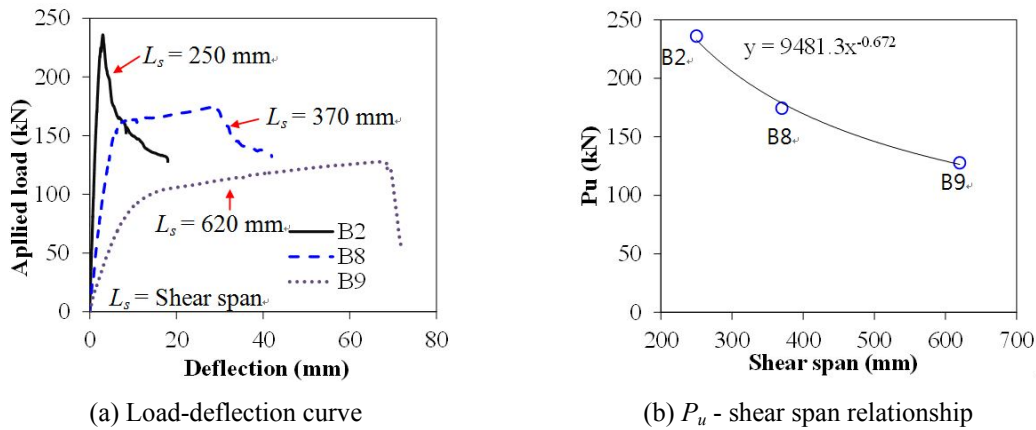


Fig. 8 Effect of shear span length

of connectors are available in the shear span to resist shear cracking. The number of connectors in the shear span has significant effect on the shear resistance of the beam.

3.2.4 Effect of shear span

Beams B2, B8, and B9 are designed with different shear span L_s (L_s is the spacing from the support center to the loading point). The effect of the shear span on the load-deflection curves and ultimate strength of the beams are shown in Figs. 8(a) and (b), respectively. Table 3 shows the maximum load carrying capacities of the beams obtained from the tests. Since the beams are subject to concentrated load(s), the most critical beam section occurs at the concentrated load point where the section is subject to combined bending moment and transverse shear force. The magnitude of the bending moment is influenced by the shear span. From Fig. 8(a), it can be seen that the failure mode of the beam changes from typical shear failure to the flexural failure when the shear span of the beam increases. For beam B8, a combined shear and flexural failure occurred because of its intermediate shear span compared with B2. The load carrying capacity reduces as the shear span increases as shown in Fig. 8(b). Beam B9 has the lowest load carrying capacity since it has the longest shear span as compared to B2 and B8.

4. Design of SCS sandwich beam

The maximum resistance of SCS beam is influenced by the behavior of shear connectors in the concrete core. The overlapped connectors provide interfacial shear transfer between the concrete core and steel face plates, and also prevent the shear cracks developed in the concrete core. In this section, the shear and tensile resistances of overlapped headed studs were firstly reviewed based on the past research. Design equations are then developed to predict the beam section resistance due to moment, shear, and combined actions of moment and high shear.

4.1 Shear resistance of connector

The design shear strength of the headed shear studs can be calculated by the following

formulae in EC4 (2004)

$$P_H = \min(0.29\alpha d^2 \sqrt{f_{ck}} E_{ck}, 0.8\sigma_u \pi d^2 / 4) / \gamma_v \quad (1)$$

where, $\alpha = 0.2 (h_s/d + 1)$ for $3 \leq h_s/d \leq 4$, $\alpha = 1$ for $h_s/d > 4$; h_s = nominal height of the connector; f_{ck} = compressive strength of concrete cylinder; E_{ck} = elastic modulus of the concrete; d = diameter; γ_v = partial safety factor as recommended in EC4 (2004); σ_u = ultimate tensile strength.

4.2 Tensile resistance of headed shear stud

Under tension, the possible failure mode of headed shear stud embedded in the concrete are (1) concrete breakout failure; (2) pullout failure; (3) tensile failure; and (4) punching shear failure of the steel plate, as shown in Fig. 9. The corresponding tensile resistances for these failure modes are summarized as follows.

4.2.1 Concrete breakout failure

General information on calculating the breakout resistance of the concrete cone is given in ACI 349 (1990). In this paper, the 45-degree cone method was used to calculate the concrete breakout resistance. The concrete breakout resistance of the pulled out concrete cone is computed by assuming of a conical failure surface with a slope of 45-degree between the failure surface and the bottom surface of the cone (Fig. 9(a)). A constant tensile stress of $0.96\sqrt{f_{ck}}$ is assumed to act on the cone shaped surface.

For a single tensile anchor, the design breakout resistance of concrete may be obtained from

$$T_{CB} = 0.333\sqrt{f_{ck}} A_N / \gamma_c \quad (2)$$

where A_N = the projected area of the cone surface to the free concrete surface, and it is influenced by the spacing of the connector in the SCS sandwich beam, $A_N = \min[\pi h_s^2 (1 + d/h_s), S \cdot S_w]$; S = spacing of the connectors in the longitudinal direction of the beam; S_w = spacing of the connectors in the width direction; d = diameter of the connector; h_s = height of the connector; f_{ck} = compressive strength of the concrete cylinder; γ_c = partial factor for concrete as recommended in EC2 (2004). All the parameters are in metric unit.

4.2.2 Pullout failure

The pullout failure of the connector is due to the compression failure of the concrete surrounding

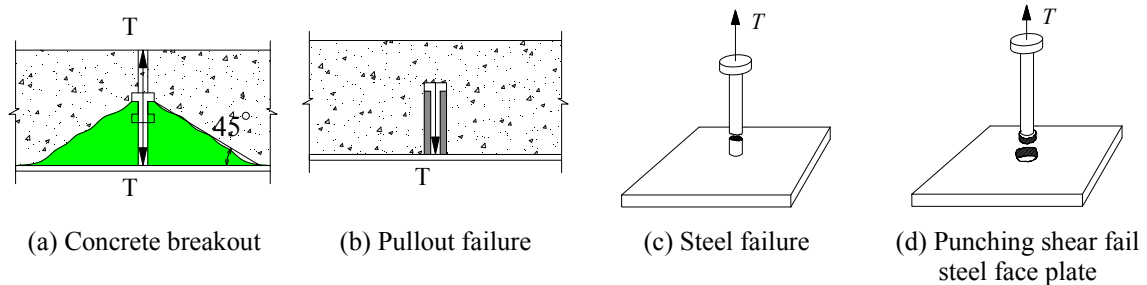


Fig. 9 Failure mode of the headed shear stud in SCS sandwich composite beam

the head of the stud as shown in Fig. 9(b). In ACI 318-08 (2008), the nominal design pullout resistance of the connector is governed by

$$T_{pl} = \psi_{c,p} T_P \quad (3a)$$

where $\psi_{c,p} = 1.4$ for connector in region without cracking at service load levels, and $\psi_{c,p} = 1.0$ for connector in region with cracking at service load levels; T_P = pullout resistance of connector.

For headed shear stud connectors, the design pullout resistance of the connector is

$$T_P = 8A_{brg}f_{ck} / \gamma_c \quad (3b)$$

where A_{brg} = bearing area of the head of stud.

4.2.3 Tensile fracture

Tensile fracture of the headed stud is shown in Fig. 9(c). The ultimate tensile resistance of the steel shank is

$$T_S = A_s f_{ut} / \gamma_{M2} \quad (4)$$

where A_s = the cross section area of the connector shank; f_{ut} = ultimate tensile strength of the stud steel material; γ_{M2} = partial factor for cross-section in tension to fracture (Eurocode 3 2005).

4.2.4 Punching shear failure of the steel face plate

The punching shear failure of the steel face plate is shown in Fig. 9d. The design punching shear resistance T_{ps} of the steel face plate to which the shear stud was attached may be calculated as (Eurocode 3 2005)

$$T_{ps} = \pi dt (f_{ys} / \sqrt{3}) / \gamma_{M0} \quad (5)$$

where d = diameter of the connector; t = thickness of the steel plate; f_{ys} = yield strength of the steel plate; γ_{M0} = partial factor for resistance of cross-section (Eurocode 3 2005).

4.2.5 Design tensile resistance

The design tensile resistance T_{hs} of the headed shear stud is determined by the smallest value of the above mentioned four resistances calculated by Eqs. (2)-(5), i.e.

$$T_{hs} = \min(T_{CB}, T_{pl}, T_S, T_{ps}) \quad (6)$$

The tensile resistance of headed studs based on the four failure modes of a sandwich composite beam with sectional width 250 mm and height of shear stud h_s varying from 20 to 250 mm are plotted in Fig. 10. It can be observed that the tensile resistance of the headed studs in the SCS sandwich composite beam is influenced by the height of the stud h_s , strength of the core material ($f_{ck} = 30, 60, \text{ and } 180 \text{ MPa}$), and spacing of the connectors ($S = 50, 100, 150 \text{ and } 200 \text{ mm}$). The followings can be concluded based on the comparisons in Fig. 10:

- For SCS sandwich composite beam with lower strength concrete e.g., $f_{ck} = 30 \text{ MPa}$ as shown in Fig. 10(a), the tensile resistance of the headed studs is controlled by the concrete breakout resistance or pullout resistance. As the strength of the concrete increases to 180 MPa for

high performance concrete, the tensile resistance of headed stud is governed by the tensile fracture resistance of the stud or punching shear resistance of the steel face plate as shown in Fig. 10 (c). For the SCS sandwich composite beam with core concrete strength of 60 MPa as shown in Fig. 10 (b), the tensile resistance of the headed stud is influenced by the spacing of the connectors and height of the shear stud.

- When the height of the headed stud is less than 80 mm (see Figs. 10(a)-(b)), the tensile resistance of connector is affected more by the concrete breakout and pullout resistance. Therefore for slim decking system, the effectiveness of headed stud to resist pullout force will be affected (see Eq. (2)). The full concrete breakout failure surface cannot be achieved due to the limited space that is formed by the dense layout of the connectors in the sandwich composite. In such case, the concrete breakout resistance of the headed stud will be controlled by the spacing of the connectors, S , and it will remain the same even though the height of the stud increases as shown in Figs. 10(a)-(c).
- Increase of connector's spacing leads to higher concrete breakout resistance due to larger breakout failure surface in the SCS sandwich composite beam. However, as the spacing between connector increases, less number of connectors is available to achieve composite action that may reduce the flexural resistance of the sandwich composite beam.

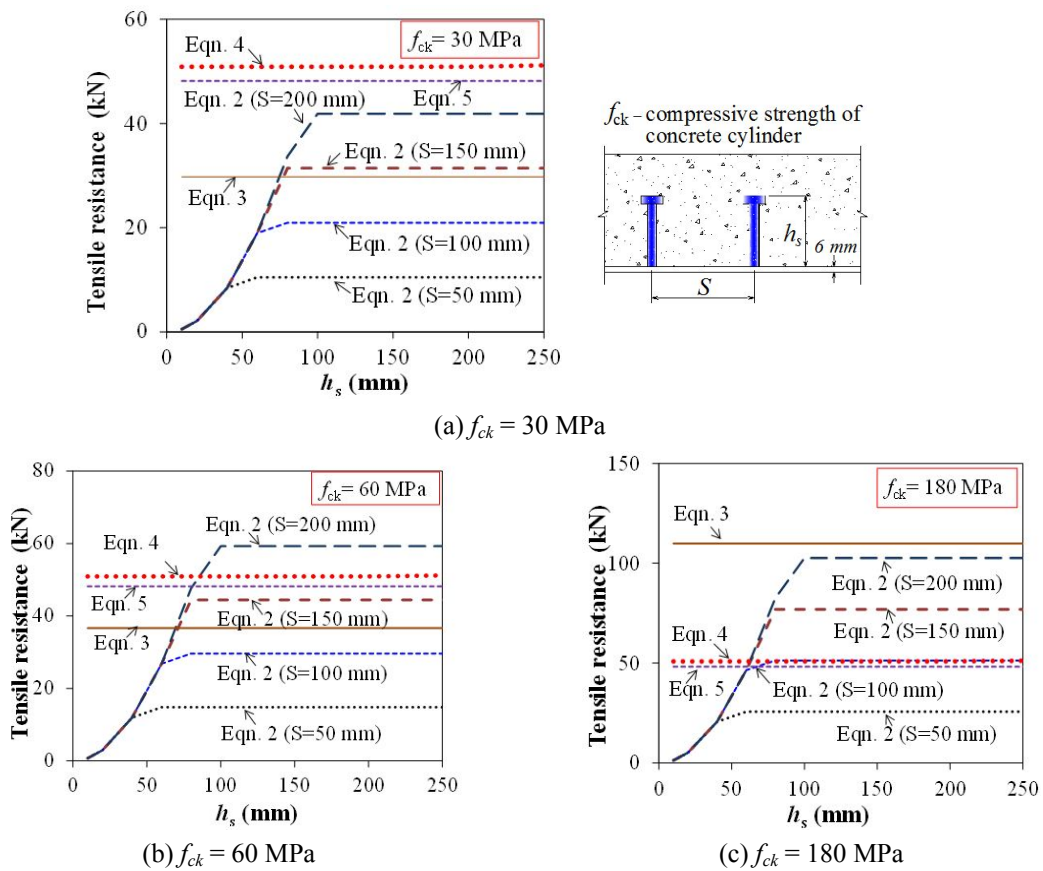


Fig. 10 Tensile resistance of the headed studs with different height

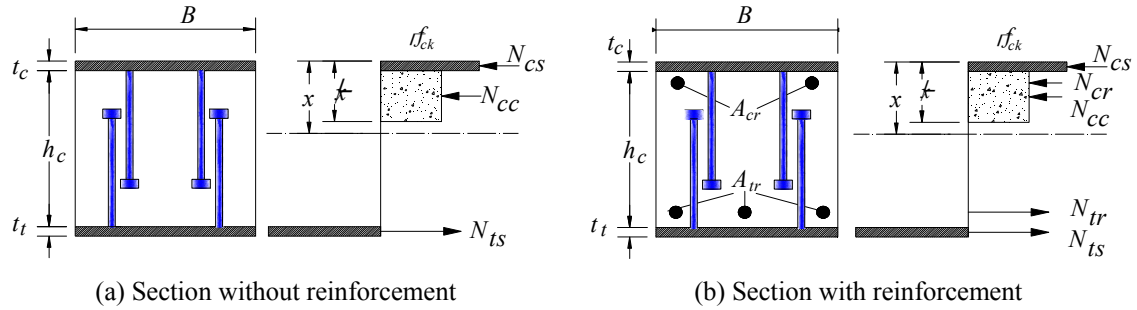


Fig. 11 Stress block of the sandwich composite beam section

4.3 Flexural resistance

Several assumptions were made for the calculation of the flexural resistance of the SCS sandwich composite beams as the following: (1) plane section remains plane; (2) contribution of tensile strength of concrete is ignored; (3) full plastic rectangular stress block can be developed in the concrete. Based on plastic analysis of cross section, the plastic stress blocks acting on a SCS section are shown in Fig. 11. The compressive strength of the concrete can be calculated as in Eurocode 2 (2004)

$$N_{cc} = \eta f_{ck} \lambda x B / \gamma_c \quad (7)$$

where B = width of the beam; x = depth of the neutral axis position as shown in Fig. 11(a); $\lambda = 0.8$ for $f_{ck} \leq 50$ MPa, $\lambda = 0.8 - (f_{ck} - 50)/400$ for $50 < f_{ck} \leq 90$ MPa; $\eta = 1.0$ for $f_{ck} \leq 50$ MPa; $\eta = 1.0 - (f_{ck} - 50)/200$ for $50 < f_{ck} \leq 90$ MPa.

The maximum force developed in the steel plate is governed by either the yield resistance of the steel plate or the shear resistance of the connectors in the compressive or tension zone of the concrete. This force can be calculated by

$$N_{cs} = \min(n_c P_s, f_{ysc} A_{sc} / \gamma_{M0}) \quad (8)$$

where n_c = number of the shear connectors in the compressive zone; P_s = shear resistance of the connectors in the compression zone; f_{ysc} = yield strength of the steel plate in compression; A_{sc} = area of the compression steel plate.

Following the same principle, the tension force in the tension steel plate could also be calculated by

$$N_{ts} = \min(n_t P_s, f_{yst} A_{st} / \gamma_{M0}) \quad (9)$$

where n_t = number of the shear connectors attached to the tension steel plate; P_s = shear resistance of the connectors attached to the tension steel plate; f_{yst} = yielding strength of the steel plate under tension; A_{st} = area of the steel plate under tension.

Based on equilibrium of tension and compression force, the depth of compression zone of concrete can be calculated by equilibrium of forces

$$N_{cc} + N_{cs} = N_{ts} \quad (10)$$

$$x = \frac{(N_{ts} - N_{cs})}{\eta f_{ck} B \lambda x / \gamma_c} \quad (11)$$

The section plastic moment resistance is obtained by taking moment about the center of the compression steel plate as

$$M_{rd} = N_{ts}(h_c + t_c/2 + t_s/2) + N_{cc}(\lambda x/2) \quad (12)$$

If steel reinforcement bars are used as shown in Fig. 11(b), their contributions to the moment resistance of SCS sandwich composite beams should be considered. Eqs. (10)-(12) may be modified as

$$N_{cc} + N_{cs} + N_{cr} = N_{ts} + N_{tr} \quad (13)$$

where $N_{tr} = f_{yr} A_{tr} / \gamma_s$ is the tensile resistance of the reinforcements in the tension region of the beam, $N_{cr} = f_{ycr} A_{cr} / \gamma_s$ is the compression resistance of the reinforcements in the compression region, A_{tr} and A_{cr} are the area of the tension and compression reinforcements, respectively; γ_s = partial factor for the reinforcement (Eurocode 2 2004).

Subsequently, the position of neutral axis in the beam section can be calculated by

$$x = \frac{(N_{ts} + N_{tr} - N_{cs} - N_{cr})}{\eta f_{ck} B \lambda x / \gamma_c} \quad (14)$$

Then, the bending moment of the beam section is calculated by

$$M_{rd} = N_{ts}(h_c + t_c/2 + t_s/2) + N_{cc}(\lambda x/2) + N_{tr}(h_c - a_t + t_s/2) + N_{cr}(t_s/2 + a_c) \quad (15)$$

where a_c and a_t = cover thickness of the concrete for the reinforcements in compression and tension zone of the beam, respectively.

4.4 Transverse shear resistance of the SCS sandwich beam

Transverse shear resistance of the SCS sandwich composite beam consists of contributions from the concrete core and shear resistance provided by the overlapped connectors as (Eurocode 4 2004, Eurocode 2 2004)

$$V_{rd} = V_c + V_s \quad (16)$$

where V_c = shear resistance of concrete; and V_s = shear resistance provided by mechanical connectors. In EC2 (2004), V_c is given by

$$V_c = [C_{Rd,c} k \eta_1 (100 \rho_1 f_{ck})^{1/3}] B h_e \quad (17)$$

where $C_{Rd,c} = 0.18 / \gamma_c$ for normal weight concrete and $C_{Rd,c} = 0.15 / \gamma_c$ for lightweight concrete; $k = 1 + \sqrt{200/h_c} \leq 2.0$ and h_c is in mm; $\eta_1 = 0.40 + 0.60u / 2200$ is the tensile strength reduction coefficient, and u is density of the lightweight concrete in kg/m^3 ; $\rho_1 = t_s / [h_c + (t_s + t_c) / 2] \leq 0.02$; t_c = thickness of the steel plate under compression; t_s = thickness of the steel plate under tension; B = width of the beam; h_e = effective height of the beam for the calculation of the shear resistance.

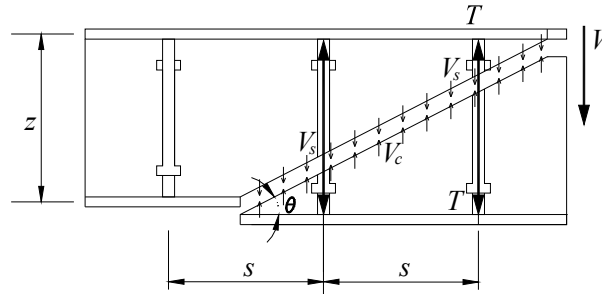


Fig. 12 Illustration of shear resistance of SCS sandwich composite beam

Considering the thickness of the steel plate, the effective depth of the SCS beam needs to be modified as

$$h_e = h_c + t_c E_s / E_c \quad (18)$$

where, h_c = height of the concrete core; t_c = thickness of the compression steel face plate; E_s = elastic Young's modulus of steel face plate; E_c = elastic secant modulus of concrete.

The shear resistance provided by the presence of headed stud connectors is calculated by

$$V_s = n_0 T z / S \quad (19)$$

where $T = T_{hs}$ = tensile resistance of a pair of overlapped headed studs embedded in concrete core by Eq. (6); S = spacing of the connectors, in mm; z = depth of the section of the SCS sandwich composite beam; T , S , z are as shown in Fig. 12.

4.5 Strength under combined bending moment and shear forces

The design equation proposed by Roberts *et al.* (1996) may be used to check the strength of beam section subject to combined action of bending and shear

$$\left\{ \frac{V}{V_{rd}} \right\}^2 + \left\{ \frac{M}{M_{rd}} \right\}^2 = R^2 \leq 1 \quad (19)$$

where V_{rd} and M_{rd} are the shear and bending resistances of the beam section, respectively; V and M are the shear force and bending moment acted on the beam section; R is the index of the strength.

The critical sections of the SCS sandwich composite beam can be judged from the bending moment and shear distribution diagram.

4.6 Elastic deflection

It was observed from the tests that the flexural stiffness of the beam was significantly influenced by the interfacial slip between the face plates and core concrete. A method to calculate the elastic deflection of a partially composite SCS sandwich composite beam is recommended by applying a reduction factor to the width of the steel face plates in case of that the number of

provided shear connectors is not adequate to achieve full composite action. The reduction factors for tension and compression plates' width are calculated as follows (Narayanan *et al.* 1994)

$$k_t = \frac{n_t K_t}{n_t K + 2Bt_t E_s / L} \quad (20a)$$

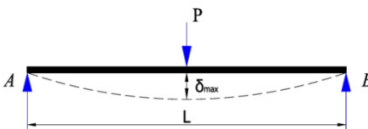
$$k_c = \frac{n_c K_c}{n_c K + 2Bt_c E_s / L} \quad (20b)$$

where B = width of the beam; n_c = quantity of the shear connectors attached to the compression steel face plate; n_t = quantity of the shear connectors attached to the tension steel face plate; E_s = elastic modulus of the steel face plate; L = span of the SCS sandwich composite beam; t_c = thickness of the compression steel face plate; t_t = thickness of the tension steel plate; K_t and K_c are the elastic stiffness of shear force-slip curves of the mechanical connectors attached to tension and compression plates, which can be obtained from push test or by the following empirical formulae (Shim *et al.* 2004)

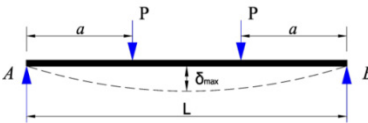
$$K = \frac{P_{\max}}{d(0.16 - 0.0017f_c)} \quad (20c)$$

where P_{\max} = ultimate shear resistance of the connectors; d = diameter of the shear connector in mm; f_c = compressive strength of the concrete in N/mm^2 . In Eq. (20c), 0.16 will be substituted by 0.24 and 0.08 for the lower and upper characteristic stiffness, respectively. It should also be noticed that Eq. (20c) has limitations on concrete strength; the f_c should be less than 67 MPa.

The central deflections of SCS sandwich composite beams under one-point or two-point loading can be calculated as follow



$$\delta = \delta_m + \delta_v = \frac{PL^3}{48D} + \frac{PL}{4S} \quad (21a)$$



$$\delta = \delta_m + \delta_v = \frac{PL^3}{6D} \left[\frac{3a}{4L} - \left(\frac{a}{L} \right)^3 \right] + \frac{Pa}{2S} \quad (21b)$$

where δ = central deflection of the beam; S = shear stiffness of the beams and calculated by Eq. (23); P = applied concentrated force; a = distance between the applied concentrated force and the end support; L = beam span; $D = E_s I_{eq}$ is the flexural stiffness of the sandwich composite section; I_{eq} = equivalent moment inertia of the cross section of SCS sandwich composite beam and is given by

$$I_{eq} = \frac{Bk_c t_c^3}{12} + Bk_c t_c \left(x_c + \frac{t_c}{2} \right)^2 + \frac{Bk_c x_c^3}{3} + \frac{Bk_t t_t^3}{12} + Bk_t t_t \left(h_c - x_c + \frac{t_t}{2} \right)^2 \quad (22)$$

In Eqs. (21a)-(21b), S is the shear stiffness of the beams given by Oehlers and Bradford (1999) as follow

$$S = \frac{G'_c h_c B}{\kappa_s} \tag{23a}$$

where κ_s = the shear factor and adopted as 1.2 for rectangular section. G'_c is the effective shear modulus given as

$$G'_c = \frac{\phi G_c}{1 + E_c h_c^2 / \left(6 E_s \left(\frac{t_t + t_c}{2} \right) e \right)} \tag{23b}$$

where $e = h_c + (t_c + t_t) / 2$ is the distance between center of the top and bottom steel face plate; $\phi = 0.95$ is shear modulus reduction factor accounting concrete crack as proposed by Oehlers and Braford (1999), and Sohel (2008).

4.7 Validation of the design equations

The validations of the design equations consist of ultimate bending resistance, transverse shear resistance, strength under combined bending moment and transverse shear, and elastic deflection under the service load.

In Eqs. (1)-(23), partial factors in Eurocodes (EC2 2004, EC3 2005, EC4 2004) were used to calculate the corresponding design resistances of J-hook connectors. However, for comparison with test results, these factors should be taken as 1,0 for the calculation of the resistance of SCS sandwich beam structure.

The predicted ultimate strength of the SCS sandwich composite beams are compared with the test results in Table 4. The bending moment M and transverse shear force V at the critical section C can be determined from the bending moment and transvers shear distribution diagrams as shown in Fig. 13. M and V are the ultimate moment and shear at the maximum load from the beam test, and M_{rd} and V_u are the predicted resistance obtained from Eq. (12) or Eqs. (15)-(16), respectively. These values are substituted into Eq. (19) to calculate the R index as shown in Table 4.

From Table 4, the average R index is 1.38 with a coefficient of variance (Cov) of 0.20. Most of the R ratio is close to 1.0 except two high R ratios of 1.70 and 1.89 for specimen B3 and B5, respectively. These high R ratios are caused by underestimating the transverse shear resistance of the beam. In these two beams, thicker steel plates and high performance concrete were used in B3

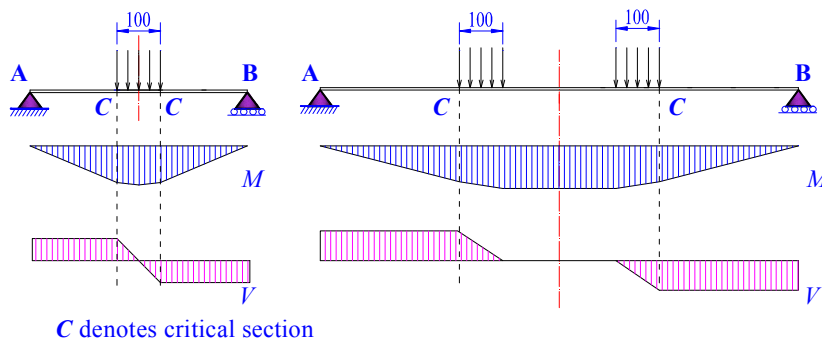


Fig. 13 Bending moment and shear distribution diagram for determination of critical section

Table 4 Ultimate strengths and failure modes of the beams B1-B9

Beam	M (kN·m)	M_{rd} (kN·m)	M / M_{rd}	V (kN)	V_{rd} (kN)	V / V_{rd}	R by Eq. (19)
	(1)	(2)	(1)/(2)	(4)	(5)	(4)/(5)	(7)
B1	21.2	22.9	0.93	106.2	97.6	1.09	1.43
B2	23.6	37.6	0.63	118.0	104.4	1.13	1.29
B3	37.8	40.8	0.93	189.0	132.2	1.43	1.70
B4	13.4	20.5	0.65	66.8	74.8	0.89	1.11
B5	45.1	40.4	1.12	225.7	147.8	1.53	1.89
B6	23.3	26.9	0.87	116.5	105.8	1.10	1.40
B7	16.5	15.5	1.07	82.7	92.8	0.89	1.39
B8	27.9	40.4	0.69	87.1	105.8	0.82	1.07
B9	36.4	40.4	0.90	63.9	104.1	0.61	1.09
Mean / Cov							1.38 / 0.20

* M = Maximum bending moment from test; M_{rd} = predicted bending moment resistance of the beam's section; V = Maximum shear force from the test; V_{rd} = predicted transverse shear resistance of the beam's section.

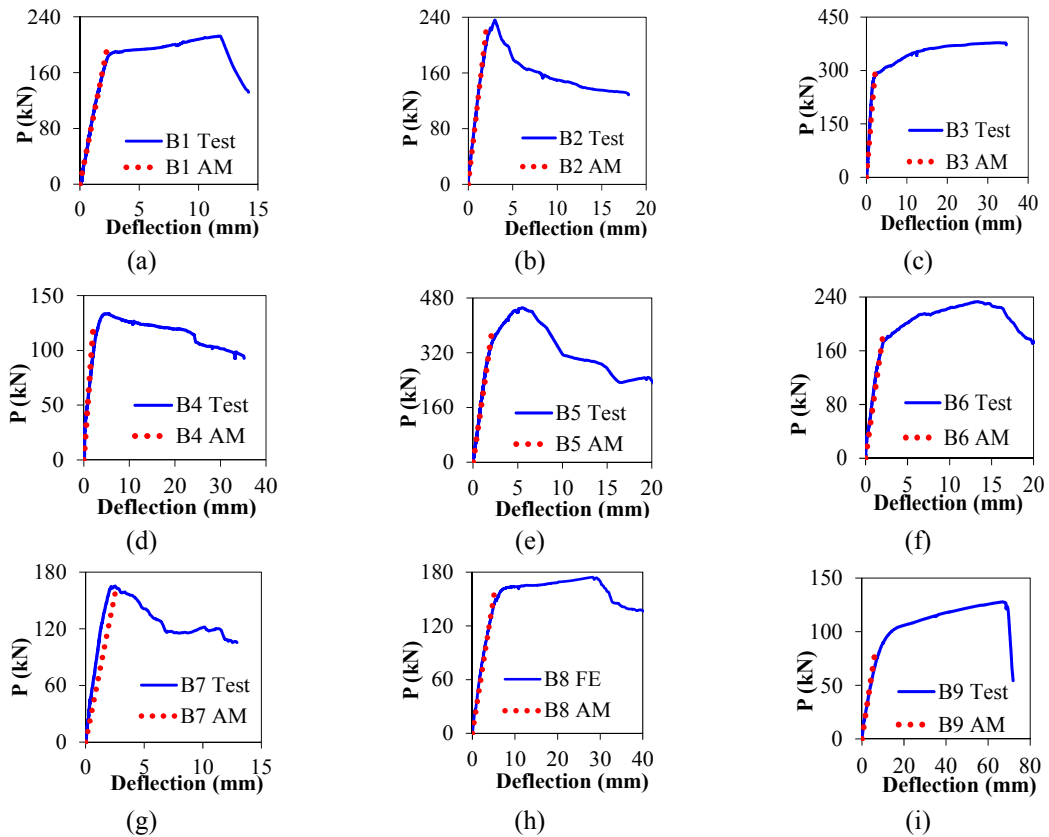


Fig. 14 Comparisons of the load-central deflection curves between test and predictions (AM denotes predictions by Eqs. (20)-(23))

and B5, respectively. This implies that the design equation needs to be further improved to account for shear resistance of high performance concrete by future experimental investigation. Nevertheless, the proposed equations lead to conservative prediction of transverse shear resistance for high strength concrete.

It is observed from Table 4 that for short span beams B1-B6 the V/V_{rd} ratio is higher than the M/M_{rd} . This implies that they failed in transverse shear mode. Beam B7 exhibited slightly higher M/M_{rd} ratio than V/V_{rd} ratio. This means that failure of B7 is governed by shear connectors' failure in which the moment resistance is limited by the shear resistance of connectors. For beam B9, it exhibits typical flexural failure as indicated by lower V/V_{rd} ratio compared to M/M_{rd} ratio. For beam B8, combined flexural failure and shear failure occurred.

The elastic load-central deflection curves predicted by Eq. (21) were compared with the experimental curves in Figs. 14(a)-(i). It can be observed that the predicted elastic load-deflection curves agree well with all the test ones with very small differences. Thus, the design equations can be used to predict the elastic deflection of the SCS sandwich composite beam under service loads.

5. Conclusions

In this paper, nine steel-concrete-steel (SCS) sandwich beams, designed with overlapped headed shear studs and new ultra-lightweight cement composite core material, were tested under static concentrated loading. Design equations were developed to predict the ultimate strength behavior of the SCS sandwich beams. From the experimental and analytical studies, the following conclusions were drawn:

- From the experimental studies, it was found that higher face plate thickness increased the flexural and transverse shear resistances of the SCS sandwich beam. Higher strength core material used in the SCS sandwich beam increased the shear and tensile resistance of the shear connector. The enhanced resistance of the connectors increased the composite action and transverse shear resistance of the sandwich beam which resulted in higher load carrying capacity of the sandwich beam. Increasing spacing of the connectors reduced the number of the shear connectors in the sandwich beam which in turn reduced the composite action. Since less connectors were available to bridge the shear cracks in the concrete core, the load carrying capacity of the beam was reduced. As the shear span of the beam increased, the failure mode changed from transverse shear type to flexure type.
- Modified design equations (Eqs. (2)-(6)) were recommended to determine the tensile resistance of the headed shear studs which may be used to determine the transverse shear resistance of composite sandwich beams. The flexural resistances of the SCS sandwich beam with and without reinforcements can be evaluated by Eqs. (12) and (15), respectively. The transverse shear resistance can be predicted by Eqs. (16)-(19). The equivalent depth of the SCS sandwich beam was redefined by Eq. (18) that considered the influence of the steel face plate. The sandwich beam's section under combined bending and transverse shear effects may be checked by Eq. (19). The elastic deflection under service loading levels of the SCS sandwich beam can be predicted by the Eqs. (20)-(23). These design equations were validated by the test results. The proposed design equations offer useful means to calculate the bending resistance, transverse shear resistance, strength of the section under combined bending moment and transverse shear, and elastic deflection under service loading.

- Through the discussions on the tensile resistance of the shear stud, it was observed the strength of the core material, height of the connector, and spacing of the connectors have significantly influenced the tensile resistance of the stud connector.

Acknowledgments

The research described herein was funded by the Maritime and Port Authority of Singapore, and supported by the American Bureau of Shipping (ABS) and National University of Singapore under research project titled “Curved steel-concrete-steel sandwich composite for Arctic region” (Project No. R-302-501-002-490).

References

- Aboobucker, M.A.M., Wang, T.Y. and Liew, J.Y.R. (2009), “An experimental investigation on shear bond strength between steel and fresh cast concrete using epoxy”, *The IES J. Part A: Civil Struct. Eng.*, **2**(2), 107-115.
- American Concrete Institute 318 (ACI) (2008), Building Code Requirements for Structural Concrete (ACI 318-08) and Commentary (ACI 318R-08), Farmington Hills, MI, USA.
- ACI 349 (1990), Code Requirements for Nuclear Safety Related Concrete Structures (ACI 349-90) and Commentary (349R-90), American Concrete Institute, Farmington Hills, MI, USA.
- ASTM A 370-05 (2005), Standard Test Methods and Definitions for Mechanical Testing of Steel Products, ASTM International, 100 Barr Harbor Drive, P.O. Box C700, West Conshohocken, PA, USA.
- Chung, K.F. and Lawson, R.M. (2001), “Simplified design of composite beams with large web openings to Eurocode 4”, *J. Constr. Steel Res.*, **57**(2), 135-164.
- Dai, X.X. and Liew, J.Y.R. (2010), “Fatigue performance of lightweight steel-concrete-steel sandwich systems”, *J. Constr. Steel Res.*, **66**(2), 256-276.
- Eurocode 2 (2004), Design of Concrete Structures – Part 1-1: General Rules and Rules for Buildings, BS EN 1992-1-1, Brussels, Belgium.
- Eurocode 3 (2005), Design of Steel Structures – Part 1-1: General Rules and Rules for Buildings, BS EN 1993-1-1, Brussels, Belgium.
- Eurocode 4 (2004), Design of Composite Steel and Concrete Structures – Part 1.1: General Rules and Rules for Buildings, BS EN 1994-1-1, Brussels, Belgium.
- Kim, S.H., Choi, K.T., Park, S.J., Park, S.M. and Jung, C.Y. (2013), “Experimental shear resistance evaluation of Y-type perfobond rib shear connector”, *J. Constr. Steel Res.*, **82**, 1-18.
- Kumar, G. (2000), “Double skin composite construction”, Master Thesis, National University of Singapore, Singapore.
- Lam, D. (2007), “Capacities of headed stud shear connectors in composite steel beams with precast hollowcore slabs”, *J. Constr. Steel Res.*, **63**(9), 1160-1174.
- Leekitwattana, M., Boyd, S.W. and Shenoi, R.A. (2011), “Evaluation of the transverse shear stiffness of a steel bi-directional corrugated-strip-core sandwich beam”, *J. Constr. Steel Res.*, **67**(2), 248-254.
- Liew, J.Y.R. and Sohel, K.M.A. (2009), “Lightweight steel-concrete-steel sandwich system with J-hook connectors”, *Eng. Struct.*, **31**(5), 1166-1178.
- McKinley, B. and Boswell, L.F. (2002), “Behaviour of double skin composite construction”, *J. Constr. Steel Res.*, **58**(10), 1347-1359.
- Mirza, O. and Uy, B. (2010), “Effects of the combination of axial and shear loading on the behaviour of headed stud steel anchors”, *Eng. Struct.*, **32**(1), 93-105.
- Narayanan, R., Roberts, T.M. and Naji, F.J. (1994), *Design Guide for Steel-Concrete-Steel Sandwich Construction, Volume 1: General Principles and Rules for Basic Elements*, SCI Publication P131, The

- Steel Construction Institute, Ascot, Berkshire, UK.
- Narayanan, R., Wright, H.D., Evans, H.R. and Francis, R.W. (1998), "Load tests on double skin composite girders", *Proceedings of International Conference on Composite Construction*, Henneker, NH, USA.
- Oduyemi, T.O.S. and Wright, H.D. (1989), "An experimental investigation into the behaviour of double skin sandwich beams", *J. Constr. Steel Res.*, **19**(2), 97-110.
- Oehlers, D.J. and Bradford, M.A. (1999), *Elementary Behaviour of Composite Steel and Concrete Structural Members*, Butterworth-Heinemann Publishing Inc., Oxford, Boston, MA, USA.
- Roberts, T.M., Edwards, D.N. and Narayanan, R. (1996), "Testing and analysis of steel-concrete-steel sandwich beams", *J. Constr. Steel Res.*, **38**(3), 257-279.
- Shanmugam, N.E. and Lakshmi, B. (2001), "State of the art report on steel-concrete composite columns" *J. Constr. Steel Res.*, **57**(10), 1041-1080.
- Shanmugam, N.E., Kumar, G. and Thevendran, V. (2002), "Finite element modeling of double skin composite slabs", *Finite Elem. Anal. Design*, **38**(7), 579-599.
- Shim, C.S., Lee, P.G. and Yoon, T.Y. (2004), "Static behavior of large stud shear connectors", *Eng. Struct.*, **26**(12), 1853-1860.
- Sohel, K.M.A. (2008), "Impact behaviour of Steel-Composite sandwich beams", PhD. Thesis, National University of Singapore, Singapore.
- Sohel, K.M.A. and Liew, J.Y.R. (2011), "Steel-concrete-steel sandwich slabs with lightweight core-static performance", *Eng. Struct.*, **33**(3), 981-992.
- Sohel, K.M.A., Liew, J.Y.R., Yan, J.B., Zhang, M.H. and Chia, K.S. (2012), "Behavior of steel-concrete-steel sandwich structures with lightweight cement composite and novel shear connectors", *Compos. Struct.*, **94**(12), 3500-3509.
- Wang, J.Y., Zhang, M.H., Li, W., Chia, K.S. and Liew, J.Y.R. (2012), "Stability of cenospheres in lightweight cement composites in terms of alkali-silica reaction", *Cement Concrete Res.*, **42**(5), 721-727.
- Wang, J.Y., Chia, K.S., Liew, J.Y.R. and Zhang, M.H. (2013), "Flexural performance of fiber-reinforced ultra lightweight cement composites with low fiber content", *Cement Concrete Compos.*, **43**(0), 39-47.
- Wright, H.D., Oduyemi, T.O.S. and Evans, H.R. (1991), "The design of double skin composite elements", *J. Constr. Steel Res.*, **19**(2), 111-132.
- Xie, M., Foundoukos, N. and Chapman, J.C. (2007), "Static tests on steel-concrete-steel sandwich beams", *J. Constr. Steel Res.*, **63**(6), 735-750.
- Yan, J.B., Liew, J.Y.R., Soheli, K.M.A. and Zhang, M.H. (2014a), "Push-out tests on J-hook connectors in steel-concrete-steel sandwich structure", *Mater. Struct.*, **47**(10), 1693-1714.
- Yan, J.B., Liew, J.Y.R. and Zhang, M.H. (2014b), "Tensile resistance of J-hook connectors used in Steel-Concrete-Steel sandwich structure", *J. Constr. Steel Res.*, **100**, 146-162.